Optics and Lasers in Engineering 107 (2018) 91–101

Contents lists available at ScienceDirect

Optics and Lasers in Engineering

journal homepage: www.elsevier.com/locate/optlaseng

A multi-camera speckle interferometer for dynamic full-field 3D displacement measurement: Validation and inflation testing of a human eye sclera

Luigi Bruno [a,b], Gianfranco Bianco [b], Massimo A. Fazio [b,c,*]

[a] Department of Mechanical, Energy and Management Engineering, University of Calabria, Via Bucci 44C, Rende, CS 87036, Italy
[b] Department of Ophthalmology, The University of Alabama at Birmingham, 1670 University Boulevard, Birmingham, AL 35294, USA
[c] Department of Biomechanical Engineering, The University of Alabama at Birmingham, 1670 University Boulevard, Birmingham, AL 35294, USA

A R T I C L E I N F O

Keywords:
Speckle interferometry
Ocular biomechanics
Ophthalmology
Mechanical characterization
Eye tissue
Time-dependent deformations

A B S T R A C T

We developed and optimized a custom dynamic Electronic Speckle Pattern Interferometer (d-ESPI) for measuring time-dependent three-dimensional (3D) surface displacements during inflation testing of ocular tissues. The 3D displacement field was resolved under dynamic loading conditions for a simplified test case of a rubber phantom and a real-world test case of the posterior sclera of a human eye. We present the optical layout and calibration procedure of the d-ESPI, and demonstrate how the displacement field can be accurately resolved for specimen deformation rates up to 6 μm/s.

1. Introduction

Mechanical stress is a causal factor in the pathogenesis of several human diseases (e.g., cardiovascular [1] tissue degradation [2], ocular [3,4]). The mechanical response to changes in the intraocular pressure (IOP) of the load-bearing collagenous tissue of the eye (i.e., cornea and sclera) is considered to play a major role in the development of ocular pathologies such as glaucoma [4], myopia [5], and keratoconus [6]. Glaucoma, currently the largest cause of permanent blindness worldwide, is characterized by progressive damage of retinal ganglion cell (RGC) axons, bundle-like structures that carry visual information from the retina photoreceptors to the brain. Damage of the RGC axons is thought to take place at the optic nerve head (ONH) at the level of the lamina cribrosa [3], a membrane-like structure that must withstand the pressure gradient between the high-pressure environment of the eye and the lower pressure retro-bulbar cerebrospinal space. Because corneosclera biomechanics modulates IOP [7] and provides structural support to the ONH [8–10], it is considered a critical factor in the development of glaucoma.

Full-field three-dimensional (3D) optical imaging techniques such as electronic speckle pattern interferometry (ESPI) [11–13], shearography [14,15], Brillouin microscopy [16], and digital image correlation (DIC) [17] have been used to characterize the mechanical response of the cornea and sclera to quasi-static and dynamic variations in IOP. Alterations in the dynamic response of the eye to IOP detected using these and other techniques have been associated with glaucoma, both experimentally [17] and clinically [18]. Using 3D-DIC, Coudrillier et al. [17] showed that the viscoelastic response of the sclera was altered in eyes from glaucomatous donors. Corneal hysteresis (CH), as measured by the ocular response analyzer (ORA), was shown to be inversely correlated with glaucoma severity [19]. Furthermore, altered circadian IOP fluctuations were observed in normal-tension glaucoma, and Asrani et al. [20] found that large fluctuations during the diurnal period were strongly associated with the rate of glaucoma progression. Libertiaux et al. [21], using 24-hour continuous IOP telemetry, showed that the IOP transient magnitude is strongly correlated with scleral rigidity. Lastly, Qu et al. [22] demonstrated that high-magnitude and high-frequency mechanical strain promotes differentiation of human contractile myofibroblasts, which are important for tissue injury-repair responses that may regulate optic nerve head biomechanics in response to IOP fluctuations.

To more accurately characterize the relationship between altered static and dynamic biomechanical properties of ocular tissue and the development of various ocular diseases, it is necessary to measure the full-field 3D surface deformations of the specimen. In ESPI, to retrieve the displacement vector of the specimen surface, the relative phase change between illumination and reference beams must be resolved, which requires the use of either more than one observation direction (i.e., more than one camera) [23] or more than one illumination direction (i.e.,

* Corresponding author.
E-mail address: massimofazio@uabmc.edu (M.A. Fazio).

https://doi.org/10.1016/j.optlaseng.2018.03.012
Received 3 December 2017; Received in revised form 3 March 2018; Accepted 13 March 2018
0143-8166/© 2018 Published by Elsevier Ltd.

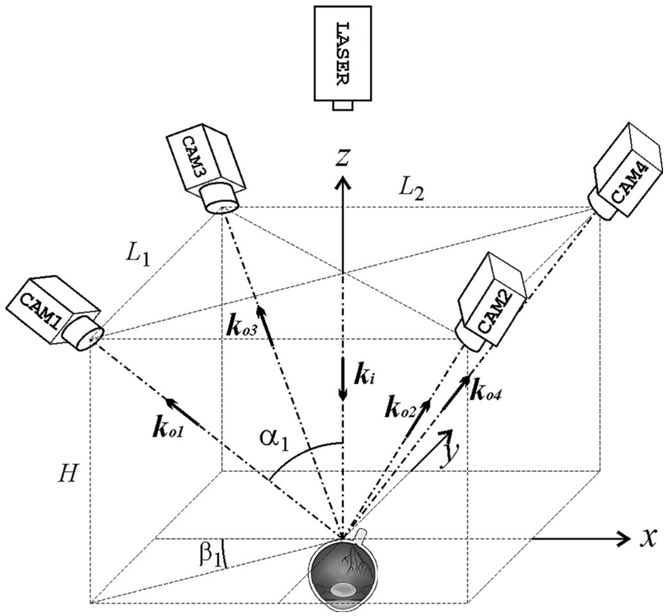

Fig. 1. Observation ($\boldsymbol{k_i}$) and illumination ($\boldsymbol{k_{o1}}, \boldsymbol{k_{o2}}, \boldsymbol{k_{o3}}, \boldsymbol{k_{o4}}$) directions imposed by the optical layout of the d-ESPI. The three lengths H, L_1, and L_2 define the sensitivity vectors. Angles α_1 and β_1 are used to calculate the sensitivity vectors for CAM1; analogous angles can be defined for the other three cameras.

by splitting and properly orienting the object beam) [24]. Less conventional approaches have been developed that are based on the use of a red-green-blue (RGB) camera [25] or more than a single laser [26,27]. For the RGB camera, three light sources with different wavelengths are required, with the Bayer filter of the camera allowing separation of the beams captured by a single charge-coupled device. For techniques using multiple lasers, the optical setup must be such that a different reference beam is obtained for each light source. Additional approaches have been recently proposed based on multiple fringe patterns corresponding to different sensitivity vectors recorded on a single interferogram [28,29], which are then separated by fast Fourier transform or other specific procedures.

In this manuscript, we describe the development, optimization, and testing of a new ESPI system capable of measuring the full-field 3D deformations of a specimen during inflation testing with dynamic IOP. This custom interferometer, referred to as dynamic ESPI (d-ESPI), was conceived to retrieve the 3D displacement vectors of a specimen's visible surface at the maximum speed allowed by the digital cameras and the lead-zirconate-titanate (PZT) actuator. We adopted an optical setup based on a single light source and four cameras symmetrically oriented around the specimen. In the d-ESPI system, the relative phase change is retrieved by a phase-shifting technique performed with a PZT actuator synchronized with the four cameras. For the displacement computation, a ray-tracing method based on the correspondence of the 3D points of the specimen surface to camera pixels matches the different phase values captured by the cameras. The procedure to calibrate the d-ESPI (sensitivity vectors) is presented in detail. The performance of the d-ESPI system to dynamically measure displacements was evaluated at different speed rates for two test cases: a rubber phantom and the posterior sclera of a human eye.

2. Material and methods

Fig. 1 shows the optical configuration of the four-camera d-ESPI system. The specimen is illuminated vertically along the z-axis by a laser and is observed from four oblique points of view. The central point of the specimen is assumed as the origin of the reference system, and the cameras observe the specimen from the four top corners of the parallelepiped HL_1L_2. The evaluation of the displacement vector $\boldsymbol{u}(x,y,z,t)$ at the time t of a generic point (x,y,z) requires measurement of the phase along at least three independent observation directions. In order to increase measurement accuracy, a linear least squares method can be applied by recording the phase of the speckle field along more than three observation directions. In this setup, we used four observations, as shown in Fig. 1. The formal relationship between the displacement vector and phases can be attained from the holographic interferometry formula [30]:

$$\begin{Bmatrix} \phi_1(x,y,z,t) \\ \phi_2(x,y,z,t) \\ \phi_3(x,y,z,t) \\ \phi_4(x,y,z,t) \end{Bmatrix} = \frac{2\pi}{\lambda} \begin{bmatrix} K_{1x} & K_{1y} & K_{1z} \\ K_{2x} & K_{2y} & K_{2z} \\ K_{3x} & K_{3y} & K_{3z} \\ K_{4x} & K_{4y} & K_{4z} \end{bmatrix} \begin{Bmatrix} u_x \\ u_y \\ u_z \end{Bmatrix} = \boldsymbol{M} \cdot \boldsymbol{u}(x,y,z,t), \tag{1}$$

where λ is the wavelength of the light source, $\phi_j(x,y,z,t)$ are the phases recorded at the time t of a generic point (x,y,z), u_x, u_y and u_z are the three components of the vector $\boldsymbol{u}(x,y,z,t)$, and $\boldsymbol{M}$ is the matrix whose rows are represented by the four sensitivity vectors $K_j = \{K_{jx}, K_{jy}, K_{jz}\}$ multiplied by the wavenumber $2\pi/\lambda$. This overdetermined linear equation system can be inverted to evaluate the three unknowns u_x, u_y and u_z as follows:

$$\begin{Bmatrix} u_x \\ u_y \\ u_z \end{Bmatrix} = \boldsymbol{M}^{+} \begin{Bmatrix} \phi_1(x,y,z,t) \\ \phi_2(x,y,z,t) \\ \phi_3(x,y,z,t) \\ \phi_4(x,y,z,t) \end{Bmatrix}, \tag{2}$$

where the superscript + indicates the pseudoinverse operation [31], which implies the application of a linear least square method to minimize the sum of squared residuals. The phase value was computed by the classical four-step temporal phase shifting procedure achieved by a PZT actuator [32]. The matching procedure that associates the phase-quadruples to the displacement of a 3D point of the specimen surface is discussed below. Referring to the Fig. 1, the sensitivity vectors are geometrically defined by:

$$\boldsymbol{K_j} = \boldsymbol{k_{oj}} - \boldsymbol{k_i} = \begin{Bmatrix} \pm\sin\alpha_j\cos\beta_j \\ \pm\sin\alpha_j\sin\beta_j \\ \cos\alpha_j \end{Bmatrix} - \begin{Bmatrix} 0 \\ 0 \\ -1 \end{Bmatrix} = \begin{Bmatrix} \pm\sin\alpha_j\cos\beta_j \\ \pm\sin\alpha_j\sin\beta_j \\ 1+\cos\alpha_j \end{Bmatrix}, \tag{3}$$

with $\alpha_j = arctan[\sqrt{L_1^2 + L_2^2}/(2H)]$; $\beta_j = arctan(L_1/L_2)$; $\boldsymbol{k_i}$ and $\boldsymbol{k_{oj}}$ unit vectors identifying illumination and observation directions, respectively; $\boldsymbol{K_j}$ sensitivity vector of the jth camera; $j = 1,\ldots, 4$. The signs in the curly brackets depend on the position of the camera with the respect of the reference system: CAM1 (–,–); CAM2 (+,–); CAM3 (–,+); CAM4 (+,+). Eqs. (1) and (2) state that the displacement accuracy depends on the geometric layout of the d-ESPI and on the phase measurements. In Section 3.1, we discuss the measurement of the sensitivity vectors by means of a static calibration procedure.

A technical drawing of the optical layout is shown in Figs. 2 and 3. For the sake of clarity, the coordinate system is consistent across the two figures according to Fig. 1. The system consists of four monochromatic PointGrey FL3-U3-13Y3M-C digital cameras equipped with a $\frac{1}{2}$-inch complementary metal oxide semiconductor (CMOS) sensor, global shutter, and USB3.0 interface, providing 1280×1024 (square) pixel resolution with size of 4.8 µm. The maximum frame rate for these cameras is 90 frames per second (fps) in full resolution mode and 150 fps in 2×2 binning mode. Ultimately, the maximum frame rate is defined by the maximum usable bandwidth provided by the USB channel. With the 2×2 binning mode enabled and a square region of interest of only ~200 pixels wide, it was possible to perform acquisitions at about 250 fps.

The phase measurement is retrieved by four-shifting the phase beam of 90°; this was performed using a Physik Instrumente (Karlsruhe, Germany) piezoelectric actuator P-752.1CD. This model is a PZT actuator with an integrated capacitive sensor, closed loop travel/resolution of